

Degradable Gelatin Microspheres as an Embolic Agent: an Experimental Study in a Rabbit Renal Model

Shinichi Ohta, MD¹
Norihsa Nitta, MD¹
Masashi Takahashi, MD¹
Kiyoshi Murata, MD¹
Yasuhiko Tabata, PhD²

Index terms:

Angiography
Microspheres
Embolism, experimental

Korean J Radiol 2007; 8: 418-428

Received August 23, 2006; accepted after revision December 27, 2006.

¹Department of Radiology, Shiga University of Medical Science, Shiga, Japan; ²Institute for Frontier Medical Sciences, Kyoto University, Kyoto, Japan

Address reprint requests to:

Shinichi Ohta, MD, Department of Radiology, Shiga University of Medical Science, Seta Tsukinowa-cho, Otsu, Shiga 520-2192, Japan
Tel. (81) 77548-2288
Fax. (81) 77544-0986
e-mail: junryuhei@belle.shiga-med.ac.jp

Objective: To investigate the basic characteristics of degradable gelatin microspheres (GMSs), including their embolic behavior and degradation periods when they are used as embolic materials in the renal arteries of rabbit models.

Materials and Methods: Based on the GMS particle size, 24 kidneys were divided into 3 groups of eight kidneys, and each group was embolized with a different GMS particle size (group 1: 35–100 μm , group 2: 100–200 μm , and group 3: 200–300 μm). From each group, two rabbits were sacrificed immediately after embolization (day 0), and a pair of rabbits from each group underwent an angiogram and were sacrificed on days 3, 7, and 14, respectively, after embolization. The level of arterial occlusion, the pathological changes in the renal parenchyma, and the degradation of the GMSs were evaluated angiographically and histologically.

Results: A follow-up angiogram on days 0, 3, 7, and 14 revealed the presence of wedge-shaped poorly-enhanced areas in the parenchymal phase as seen in all groups. The size of these areas tended to increase with the particle diameter, and persisted up to day 14. On days 3, 7, and 14, parenchymal infarctions were observed histologically in all cases, and this observation corresponded with the parenchyma being supplied by the embolized arteries. GMSs of group 1 mainly reached the interlobular arteries, while those of group 3 mainly reached the interlobar arteries. In all but two cases, the GMSs were identified histologically even on day 14, and sequential degradation was histologically identified in all GMS groups.

Conclusion: GMSs can be used as degradable embolic materials which can control the level of embolization.

Transcatheter arterial embolization (TAE) has been widely accepted for its efficacy and is used to treat various diseases, including tumors, vascular lesions, and hemorrhages (1–3). Along with advances in this technique, various embolic materials have been developed and utilized (4–7). Among these materials, gelatin sponges are the most popular and are frequently used in Japan because they are easy to handle and inexpensive. Additionally, other embolic materials such as polyvinyl alcohol and trisacryl gelatin microspheres are not commercially available in Japan (8). However, since gelatin sponges require manual cutting, the sizes of the fragments are not uniform. Hence, it is impossible to intentionally select the occlusion level of the vessels. Furthermore, although they are believed to degrade in the vessels within a few weeks, the degradation periods of these sponges cannot be strictly controlled (9, 10).

Gelatin microspheres (GMSs) are products that were originally developed by Tabata

in 1987 for use as drug delivery systems (DDSs) (Fig. 1) (11–16). Gelfoam powder (Upjohn, Tokyo, Japan) is widely known as being composed of gelatin particles and is commercially available.

However, since Gelfoam powder is made by simply milling gelatin sponges, its shape is irregular and size is varied. Therefore Gelfoam powder is not classified in the category of microspheres (17). Moreover, as in the case of Gelfoam, the degradation period of Gelfoam powder cannot be controlled.

In contrast, GMSs are manufactured by an entirely different process. GMSs are spherical, and their degradation period and diameter can be controlled. These properties may be beneficial for their use as embolic materials. Although Gelfoam can degrade completely within approximately one month in the extravascular tissue and within a few weeks in the vascular space (9, 10, 18), whether or not GMSs degrade more quickly within the vascular space than in the extravascular space is unknown. Moreover, whether or not the level of occlusion is controlled in parallel with the size of GMSs is also unknown. This study aims at determining the basic characteristics of GMSs, including their embolic behavior and the degradation period when they are used as embolic materials in the renal arteries in rabbit models.

MATERIALS AND METHODS

Materials

Acidic gelatin (MW, 99 kDa) with an isoelectric point of 5.0 was obtained from Nitta Gelatin Co. Ltd., Osaka, Japan. All other chemicals used were of the highest purity available commercially.

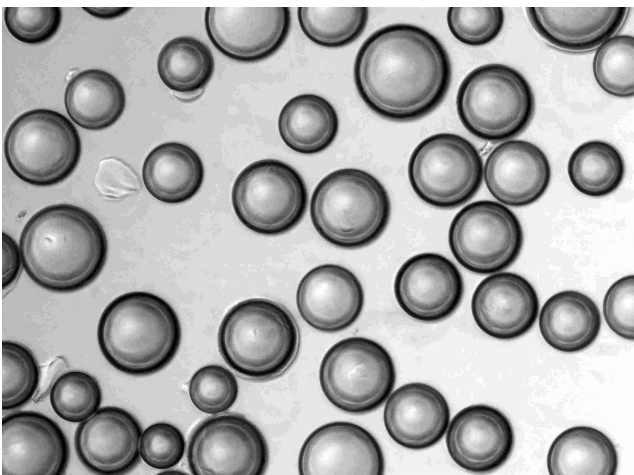


Fig. 1. Microscopic appearance of gelatin microspheres (original magnification, $\times 100$). Gelatin microspheres are spherical in shape when dispersed in double-distilled water.

Preparation of Gelatin Micorpheres

Gelatin micorpheres were prepared according to the modified method of Tabata and Ikada (1989) by glutaraldehyde crosslinking of an aqueous gelatin solution dispersed in an oil phase in the absence of a surfactant (12). In brief, 10 ml of acidic aqueous gelatin solution (10%) that was preheated to 37°C was added dropwise into 375 ml of olive oil (Wako Pure Chemical Industries, Ltd., Osaka, Japan), and the mixture was stirred at 400 rev min^{-1} at 37°C for 10 min to yield a water-in-oil (w/o) emulsion. The stirring was continued for 30 min at 4°C , and the microspheres that were formed were washed three times with acetone (Wako Pure Chemical Industries, Ltd., Osaka, Japan) by centrifugation (5000 rev min^{-1} , 5 min, 4°C). After air drying, the microspheres were sized by passing them through sieves with different apertures (35, 100, 200, and $300\ \mu\text{m}$); they were then placed into 3 groups (group 1: 35–100 μm , group 2: 100–200 μm , and group 3: 200–300 μm) based on the sphere size.

The non-crosslinked dry GMSs were dispersed in 5 ml of an aqueous glutaraldehyde solution (7.5 mg/ml, 25%, NACALAI TESQUE Inc., Kyoto, Japan) at 4°C for 15 hr to facilitate crosslinking. The microspheres were further agitated in 5 ml of 10 mM aqueous glycine solution (NACALAI TESQUE Inc., Kyoto, Japan) at 37°C for 1 hr to block the residual aldehyde groups of the unreacted glutaraldehyde. The resulting microspheres were finally washed three times with double-distilled water by centrifugation and were freeze-dried. The GMSs used in this experiment were designed to degrade completely within seven days in the extravascular tissues (19 and unpublished data).

Embolization of the Renal Artery

The study protocol was approved by the Animal Experimentation Committee, and the experiments were performed according to the Animal Care Guidelines of Shiga University of Medical Science.

In this study, 24 kidneys of 18 female rabbits that weighed 2.5–3 kg were used. Left kidneys were basically used; however, right kidneys were also used when a left kidney was not selected easily or when bilateral kidneys were needed. These kidneys were divided into 3 groups—group 1: GMSs of 35–100 μm , $n = 8$; group 2: GMSs of 100–200 μm , $n = 8$; and group 3: GMSs of 200–300 μm , $n = 8$ —based on the diameter of the GMS particles used for embolization.

General anesthesia was administered intramuscularly to each rabbit by using medetomidine hydrochloride (0.1 mg kg^{-1} , Domitor; Meiji Seika Co., Ltd., Tokyo, Japan) and ketamine hydrochloride (25 mg kg^{-1} , Ketalar50; Sankyo

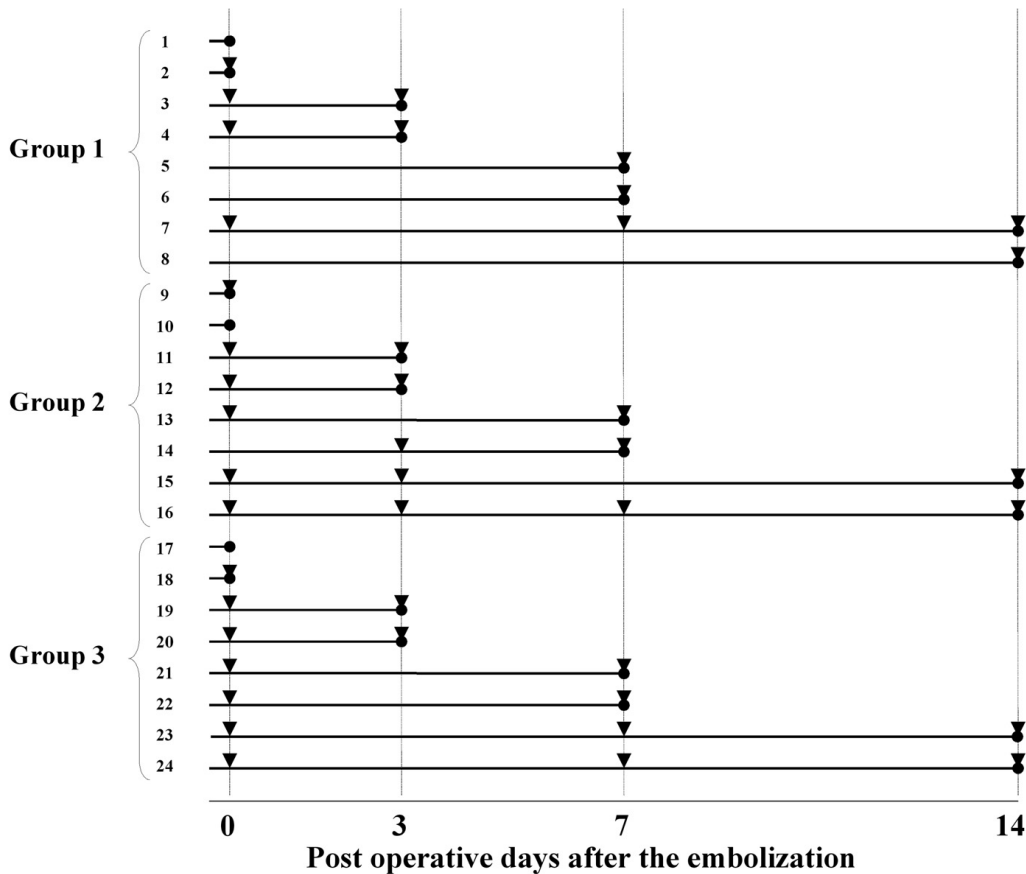
Yell Yakuhin Co., Ltd., Tokyo, Japan). The right femoral artery was surgically exposed, and a 4-Fr sheath (Clinical Supply Co., Ltd., Gifu, Japan) was inserted using a cut-down method under fluoroscopy. The trunk of the renal artery was selected using a 4-Fr cobra-type catheter (Clinical Supply Co., Ltd., Gifu, Japan), and renal arteriography was performed by manual injection of 2 ml Iopamidol (Iopamiron 370; Nihon Schering Co., Ltd., Osaka, Japan), diluted by 50%. The renal artery was embolized immediately after the administration of a mixture of 5 mg GMSs and 2 ml Iopamidol diluted by 50%.

For each GMS group, angiographies were performed in two kidneys immediately after the embolic procedure and in two kidneys each on days 3, 7, and 14 after embolization. The frequency at which sequential angiography was performed for the same kidney during the course of the experiment was as follows: 2 times, n = 10; 3 times, n = 4; and 4 times, n = 1. In six kidneys, the angiographies were performed only once during the observation period. The sequential course of the angiography of each kidney is presented in Table 1.

Analysis

Immediately after the angiogram, the rabbits were sacrificed by injecting the heart with an overdose of pentobarbital (Nembutal; Dainippon Sumitomo Pharmaceutical Co., Ltd., Tokyo, Japan), and the kidneys were surgically removed. The sequential course of the angiography and the sacrifice procedure followed for each kidney are presented in Table 1. For one kidney in each group, the rabbit was sacrificed immediately after the embolization, i.e., no angiogram was performed. This was done to observe the distribution of the GMSs immediately after embolization, thus excluding the effect of the angiographic procedure. Angiographies of renal artery were analyzed on X-ray film. These analyses focused mainly on the sizes of the poorly-enhanced areas. Since the thickness of the renal cortex was approximately 7 mm as seen on the X-ray film, poorly-enhanced areas with diameters less than 7 mm were defined as embolized areas of the interlobular artery. Therefore, poorly-enhanced areas with diameters less than 7 mm were defined as small, and those areas with diameters greater than 7 mm were defined as large. The angiograms were interpreted by two board-certified radiologists by consensus.

Table 1. Sequential Courses of Angiography (▼) and Sacrifice Procedure (●)



Embolitic Degradable Gelatin Microspheres in Rabbit Renal Model

The extracted kidneys were fixed in 10% formaldehyde solution, processed, and embedded in paraffin. Coronal histological sections were obtained, and hematoxylin and eosin (H & E) staining was performed. The pathological changes in the renal parenchyma and the level of the artery occlusion, both of which were caused by the GMSs, were evaluated based on the microscopic findings of the specimens. The pathological analyses were mainly focused on the ischemic changes in the renal parenchyma and the secondary changes in the vessel wall. The level of the renal artery occlusion caused by the GMSs was first categorized as interlobar, arcuate, and interlobular, and it was then evaluated. The occlusion level of the renal artery was determined as follow; first, the arcuate artery was identified, since it coursed along the outer side of the renal medulla. Second, the artery which coursed outer than the arcuate artery was identified as the interlobular artery. Third, the artery which coursed inner than the arcuate artery was identified as the interlobar artery.

The degradation of the GMS particles within the vessel was histologically evaluated using the following 4-point grading scale. Grade 0: the original spherical shape and size of the particle is maintained, or a slight deformation and a small cleft or cavity formation are observed within the particle without an obvious reduction in the particle size. Grade 1: size reduction and distortion of the particle and cleft or cavity formation within the particle are

moderately evident. Grade 2: size reduction and distortion of the particle and the cleft or cavity formation are clearly evident. Grade 3: GMSs are not observed in the specimens. It is speculated that GMSs completely degraded.

The histopathological analysis was preformed by two radiologists by consensus, in consultation with a pathologist.

RESULTS

Embolization Effect: Angiographic Findings

Embolization was successfully performed in all of the rabbits. The mean diameter of the renal trunk was 2.0 mm (range, 1.5–2.6 mm). The angiogram obtained immediately after embolization revealed that the nephrograms in the parenchymal phase were heterogeneous, and wedge-shaped poorly-enhanced areas were observed in four of the 17 kidneys. A follow-up angiogram on each day (performed 3, 7, and 14 days after embolization) revealed the persistence of the wedge-shaped poorly-enhanced areas in the parenchymal phase in all groups. The sizes of the poorly-enhanced areas on the angiogram are summarized in Table 2. In group 1, four out of six cases showed small, poorly-enhanced areas in the follow-up angiogram, although two out of six cases showed large areas (Fig. 2A). Among the six cases in group 2, there was

Table 2. Summary of the Angiographic and Pathological Findings

Group 1	1	2	3	4	5	6	7	8
Day after the embolization	0	0	3	3	7	7	14	14
Size of the poorly enhanced area	–	–	large	mainly small	mainly small	mainly small	small	mainly large
Occlusion level on the pathology	interlobar	interlobar-interlobular	interlobar-interlobular	interlobar-interlobular	interlobular	arcuate-interlobular	interlobular	interlobar-interlobular
Group 2	9	10	11	12	13	14	15	16
Day after the embolization	0	0	3	3	7	7	14	14
Size of the poorly enhanced area	–	–	small and large in halves	small and large in halves	mainly large	small and large in halves	small	large
Occlusion level on the pathology	interlobar	interlobar	interlobular	interlobar-interlobular	arcuate-interlobular	interlobar-interlobular	interlobular	interlobar-interlobular
Group 3	17	18	19	20	21	22	23	24
Day after the embolization	0	0	3	3	7	7	14	14
Size of the poorly enhanced area	–	–	large	large	large	large	large	large
Occlusion level on the pathology	interlobar	interlobar	interlobular	interlobar-arcuate	none	interlobular	interlobar-interlobular	none

one case of small (≤ 7 mm), poorly-enhanced areas; two cases of large areas (> 7 mm); three cases of mixed-size areas (< 7 mm or ≥ 7 mm) (Fig. 2B). In group 3, all cases showed large areas (Fig. 2C). These areas were also observed on day 14.

Embolization Effect: Pathological Findings

The level of renal artery occlusion caused by the GMSs was identified based on the pathological specimens; these values and the sizes of the poorly-enhanced areas observed in the angiograms are summarized in Table 2. It was observed that immediately after embolization, the GMSs of group 1 mainly reached the interlobular arteries, while those of group 3 mainly reached the interlobar arteries (Fig. 3). However, on days 3, 7, and 14, the GMSs with

larger diameters mainly occurred in the interlobular arteries. In group 1, agglutinated GMSs that blocked the vascular lumen occurred in the interlobar artery. On days 3, 7, and 14, parenchymal infarctions were observed in all cases; these infarctions corresponded to the feeding areas of the occluded arteries. Large infarctions were observed in the cases in which the central arteries were occluded, and these infarctions were observed on the angiogram as a large poorly-enhanced area.

In all cases, the pathological specimens showed leukocyte infiltration in the vascular walls throughout the observation period, except immediately after embolization. This infiltration was localized in the vessels where the GMSs were lodged (Fig. 4). The degree of fibrosis was more prominent on day 14 than on days 3 and 7. In group

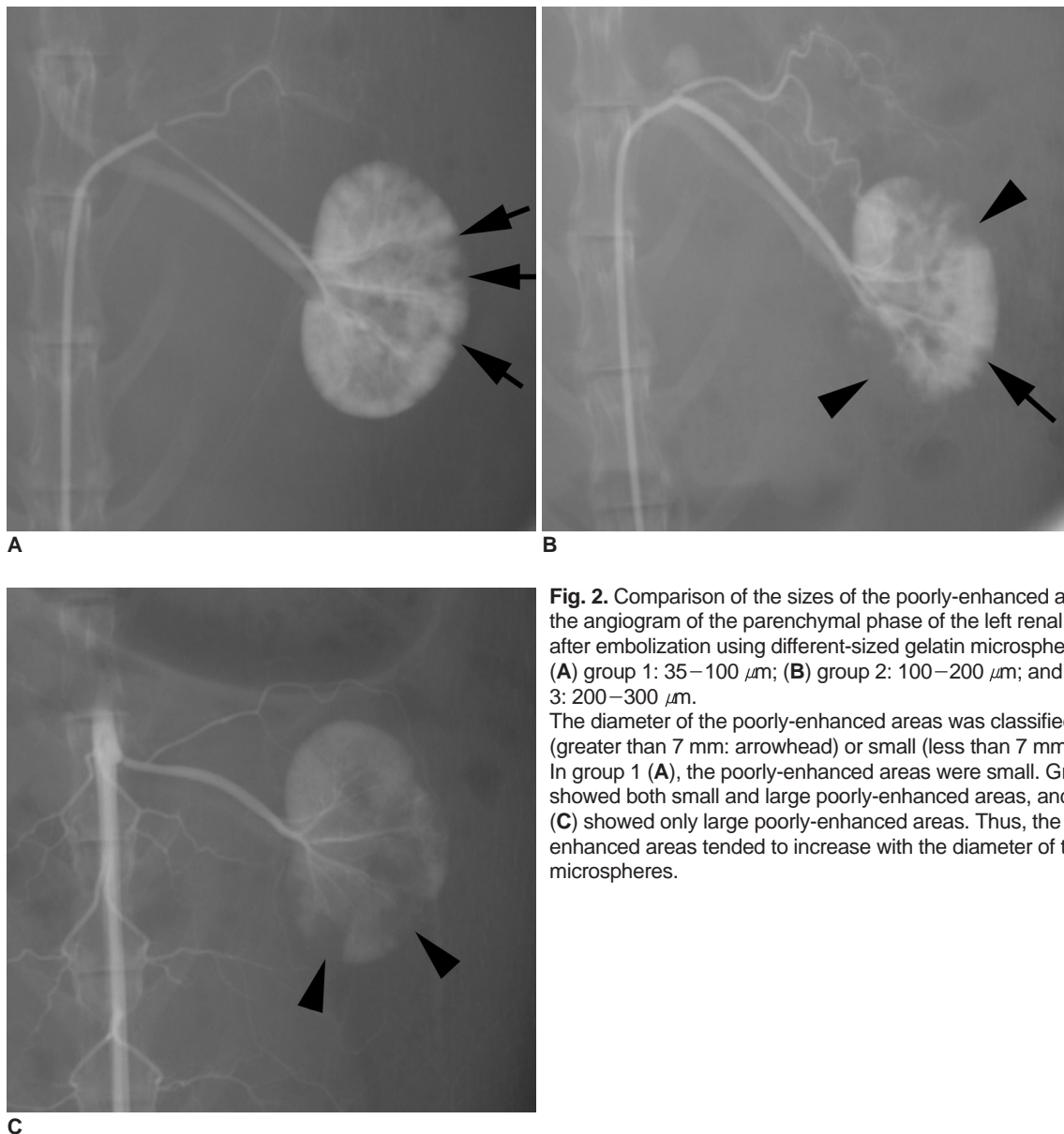


Fig. 2. Comparison of the sizes of the poorly-enhanced areas in the angiogram of the parenchymal phase of the left renal artery after embolization using different-sized gelatin microspheres. (A) group 1: 35–100 μm ; (B) group 2: 100–200 μm ; and (C) group 3: 200–300 μm .

The diameter of the poorly-enhanced areas was classified as large (greater than 7 mm: arrowhead) or small (less than 7 mm: arrow). In group 1 (A), the poorly-enhanced areas were small. Group 2 (B) showed both small and large poorly-enhanced areas, and group 3 (C) showed only large poorly-enhanced areas. Thus, the poorly-enhanced areas tended to increase with the diameter of the gelatin microspheres.

Embolic Degradable Gelatin Microspheres in Rabbit Renal Model

Table 3. Grading of Gelatin Microspheres Degradation

Group 1	3	4	5	6	7	8
Day after the embolization	3	3	7	7	14	14
Grade	0	0	1	1	2	2
Group 2	11	12	13	14	15	16
Day after the embolization	3	3	7	7	14	14
Grade	0	0	1	1	1	2
Group 3	19	20	21	22	23	24
Day after the embolization	3	3	7	7	14	14
Grade	0	0	3	1	2	3

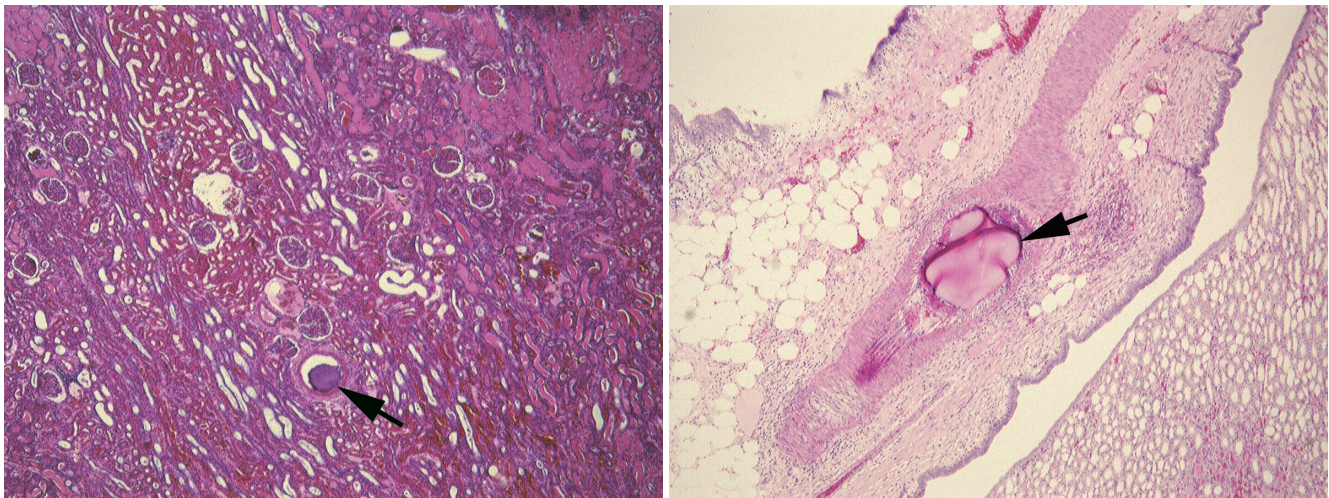


Fig. 3. Photomicrographic appearance of a resected kidney of group 1 (A) and group 3 (B) immediately after the embolic procedure. It was observed that the gelatin microspheres in group 1 frequently reached the interlobular arteries (arrow in A), while those of group 3 reached the interlobar arteries (arrow in B). (Hematoxylin & Eosin staining; original magnification, $\times 40$)

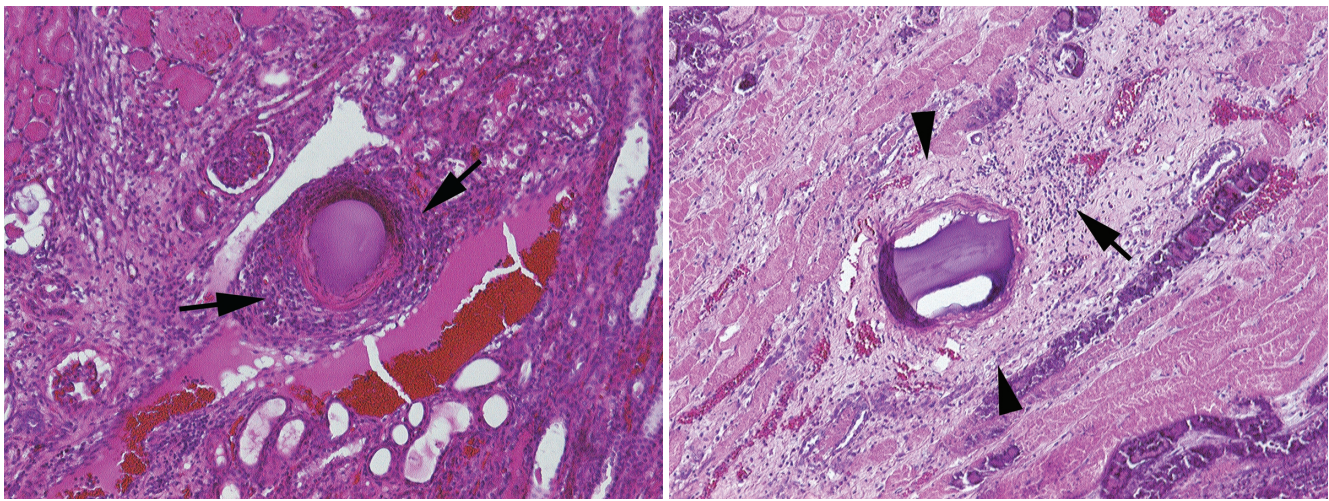


Fig. 4. Photomicrographic appearance of the secondary changes in the vessel walls of group 1.
A. Severe infiltration of leukocytes (arrows) that surrounded the gelatin microspheres was observed in the arcuate artery on day 3. Infarction of the renal parenchyma around this artery was demonstrated.
B. Fibrosis (arrowheads) was observed in the wall of the interlobar artery around the gelatin microspheres on day 14; a decrease in the number of leukocytes was also observed (arrow). These reactions were similar to those caused by Gelfoam. (Hematoxylin & Eosin staining; original magnification, $\times 100$)

1, a fibrotic change was observed in the vascular wall at the level of the interlobular artery even in the early stage of the observation period. However, in group 3, a fibrotic change was observed in the proximal portion of the renal artery; in the late stage of the observation period; this change tended to peripherally shift to the level of the interlobular arteries.

Degradation Period: Angiographic Findings

Sequential angiographic findings were obtained throughout the experiment (14 days) for five kidneys in five cases (cases 7, 15, 16, 23, and 24). In case 7 (group 1), the interlobular arteries were reperused to a greater extent on day 14 than on day 7 (Fig. 5). In case 16 (group 2), the interlobular arteries were reperused to a greater extent on

day 14 than on day 3. However, no reperfusion of the interlobular arteries was observed in cases 15 (group 2), 23 (group 3), and 24 (group 3).

Degradation Period: Pathological Findings

In all but two cases, the remnant GMSs could be histologically identified even on day 14. However, as shown in Table 3 and Figure 6, the sequential degradation of the GMSs was clearly observed. On day 3 of follow-up, the degradation level in all groups was found to be grade 0. On day 7 of follow-up, the degradation level observed in most histological findings was of grade 1. The size of the particles decreased, and mild distortion was observed. Cleft or cavity formation was observed within the particles. On day 14, it was observed that the size of the

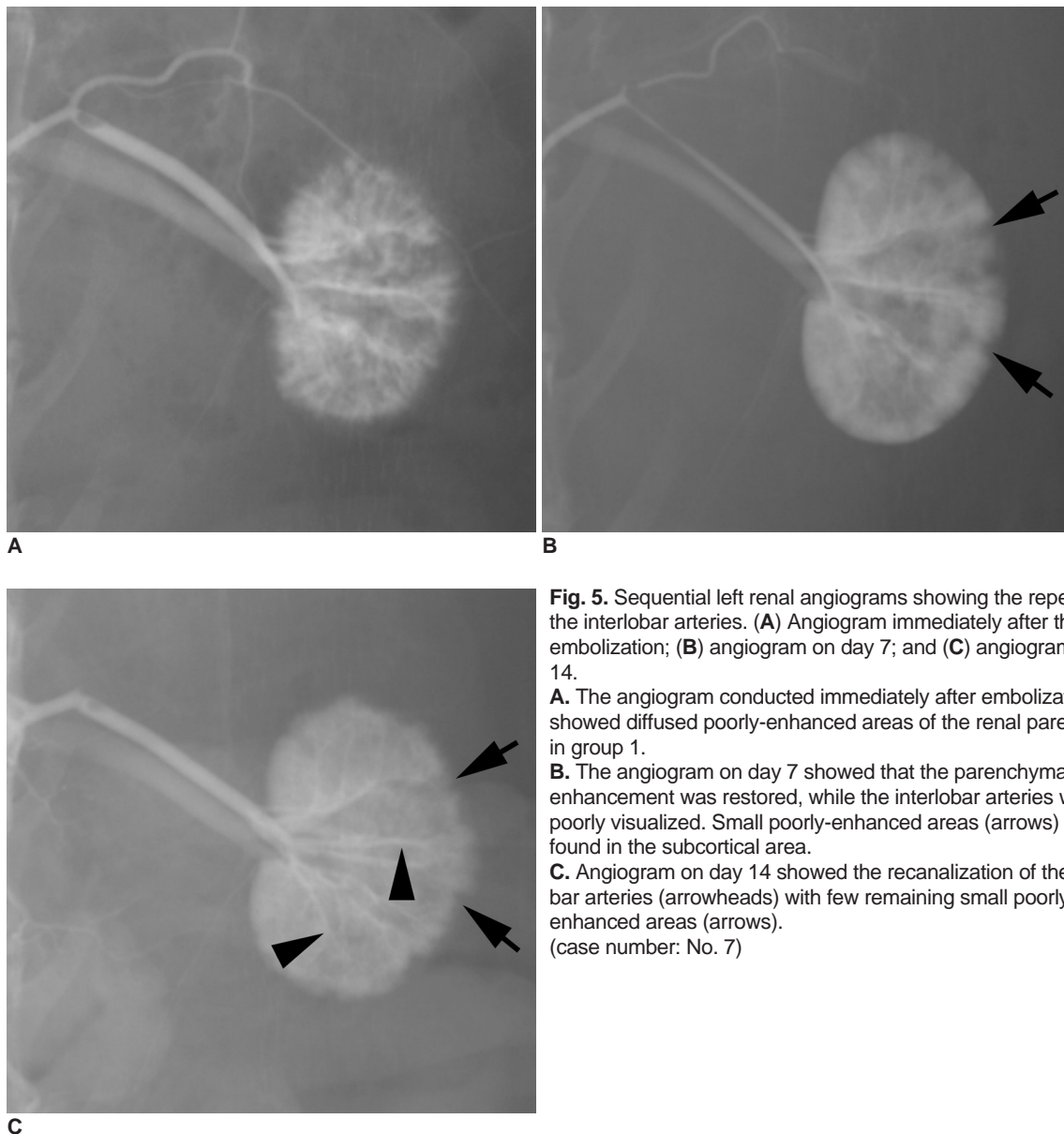


Fig. 5. Sequential left renal angiograms showing the reperfusion of the interlobular arteries. (A) Angiogram immediately after the embolization; (B) angiogram on day 7; and (C) angiogram on day 14.

A. The angiogram conducted immediately after embolization showed diffused poorly-enhanced areas of the renal parenchyma in group 1.

B. The angiogram on day 7 showed that the parenchymal enhancement was restored, while the interlobular arteries were still poorly visualized. Small poorly-enhanced areas (arrows) were also found in the subcortical area.

C. Angiogram on day 14 showed the recanalization of the interlobular arteries (arrowheads) with few remaining small poorly-enhanced areas (arrows). (case number: No. 7)

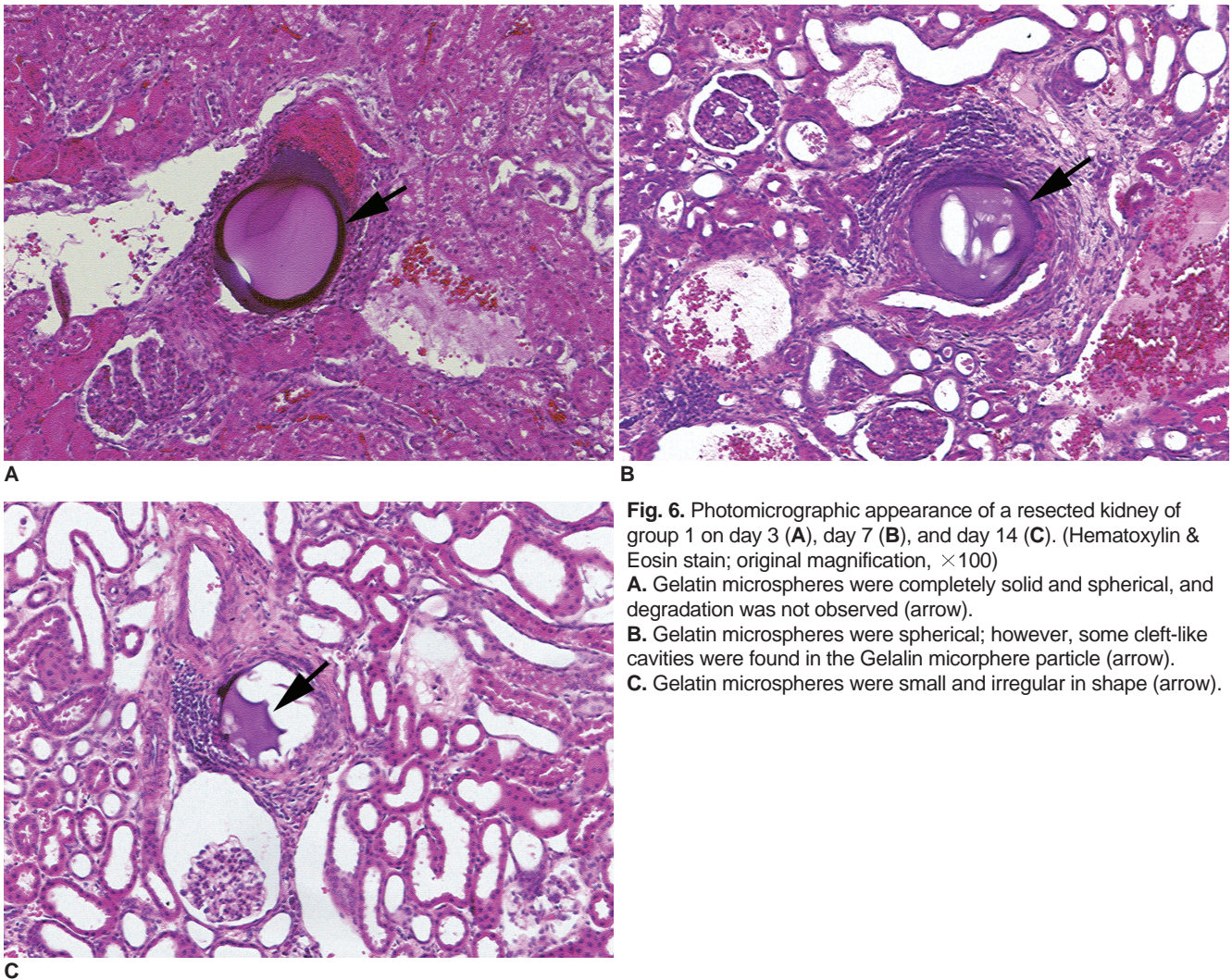


Fig. 6. Photomicrographic appearance of a resected kidney of group 1 on day 3 (A), day 7 (B), and day 14 (C). (Hematoxylin & Eosin stain; original magnification, $\times 100$)
A. Gelatin microspheres were completely solid and spherical, and degradation was not observed (arrow).
B. Gelatin microspheres were spherical; however, some cleft-like cavities were found in the Gelatin micropheer particle (arrow).
C. Gelatin microspheres were small and irregular in shape (arrow).

particles had decreased continuously and their shape was irregular. This sequential change was observed in all GMS groups.

DISCUSSION

Of the various embolic materials, gelatin sponges are most frequently used for TAE in Japan, particularly following the chemolipiodolization procedure for hepatocellular carcinoma, and to treat hemorrhage in various organs. However, reperfusion is frequently observed within a few weeks (9, 10). Although this is detrimental to embolization, it is advantageous with regard to repeated TAE for controlling tumor growth (8, 20). In such cases, repeated TAE concomitant with anticancer drug therapy would be effective. Reperfusion also contributes to the preservation of normal tissue in the embolized area. However, gelatin sponges must be cut or fragmented into small pieces with scissors and graters; this process is time consuming, and the

size of the obtained particles is not uniform. The minimum size of the obtained particles is usually limited to $500 \mu\text{m}$ (8). Thus, the success of TAE depends on the size of the gelatin sponge particles and the hands-on skills of the surgeon.

GMSs are available in a variety of sizes ranging from 10 to $500 \mu\text{m}$; an intentional size can be selected, and the particles can be generated accordingly. Additionally, in theory, the degradation period can be controlled to range from 3 days to permanent by changing the degree of crosslinking (19 and unpublished data). Thus, GMSs have the potential to embolize vessels to an intentional occlusion level if the appropriate particle size is selected; further, GMSs can control the embolic period temporarily to permanently, depending on the purpose. Tabata and colleagues have also attempted to apply GMSs in a DDS in the field of tissue engineering, and they have confirmed that GMSs can release many agents such as basic fibroblast growth factor in the target tissue (11–16). A variety of

physiochemical interactions occur between GMSs and these agents, and the agents can be released as the GMSs degrade. If the GMSs are used as the embolic material functioning as a DDS for the neoplasm, in theory, they will be significantly efficient in releasing anticancer drugs and in obliterating the feeding arteries to the intentional extent. Knowing the degradation period will enable one to prepare a time schedule for a repeated TAE and will facilitate the estimation of the degree of ischemic damage that will occur in the normal tissue present in the embolized area. In this study, based on the particle diameter, we categorized GMSs into 3 groups—35–100 μm , 100–200 μm , and 200–300 μm . We evaluated the differences among these groups with respect to the level of embolism in the vessels and the effects observed from the sequential angiographic and pathological findings. In this study, the degradation period of the GMSs in the subcutaneous tissue was set at seven days by controlling the degree of crosslinking. However, as mentioned previously, the degradation period of GMSs in the vascular space is unknown. Another important issue that we encountered in this study was whether the degradation period of the GMSs in the extravascular space can be extrapolated to those within the vascular space. The results of the angiographic and pathological findings revealed that the GMSs of all sizes had an adequate embolic effect. The size of the poorly-enhanced areas seen on the angiogram tended to increase with the particle diameter. It was also revealed that the smaller GMSs could reach the peripheral area. Further, it was pathologically proven that GMSs with a diameter ranging from 35–100 μm reached the interlobular artery, while GMSs larger than 100 μm were trapped at the level of the interlobar artery; these findings corresponded well with the angiographic findings. However, in two of six cases in group 1, which had particles of the smallest diameters, a large area of infarction was observed in the angiograms on all three days of follow-up. This discrepancy cannot be explained appropriately; however, our speculation is as follows. It is generally known that the water repellency of smaller particles tends to increase when dried particles are dispersed in water. This is because the intermolecular force between the particles is stronger than that between water molecules (21). Consequently, GMSs smaller than 100 μm tend to remain undispersed in water. Moreover, based on our experience, GMSs smaller than 100 μm tend to agglutinate easily even if they are well dispersed. The reason behind this phenomenon is unclear. However, we hypothesize that a variety of factors are intricately related, such as the Derjaguin-Landau-Verwey-Overbeek (DLVO) theory, which accounts for the dispersion and agglutination of the

molecules in water; the property of biopolymeric materials; and the surface charge (22). It was speculated that to prevent particle agglutination, the small GMS particles should have been injected after adequately dispersing them in a large amount of water. However, this injection method may pose a disadvantage to the use of GMSs.

The pathological changes in the vascular wall that were caused by the GMSs were similar to those caused by Gelfoam. Goldstein and colleagues have reported that Gelfoam embolization results in panarteritis that is characterized by the infiltration of inflammatory leukocytes into all the layers of the vessel wall as well as the disruption of the intima and the elastic tissue (23). In this study, these pathological changes were observed with GMSs of all sizes. An inflammatory reaction was observed mainly in the early observation phase; in the late phase, it changed to a fibrotic reaction. However, the degree of these changes was mild, and there was no significant difference in the severity between the GMS particles and Gelfoam.

The poorly-enhanced areas on the nephrograms remained unchanged during the sequential observation. This observation is probably related to the fact that the renal artery is an end artery. Even if the GMSs subsequently degraded after the embolization and reperfusion of the vessel, renal infarction was already established and irreversible.

GMSs larger than 100 μm were localized in the interlobar arteries immediately after embolization; however, on day 3, they were localized in the interlobular arteries. These observations revealed that the GMSs gradually migrated from the proximal to the distal portion of the artery. This was not observed in the case of the GMSs of 35–100 μm diameters because these particles had already reached the level of the interlobular artery immediately after embolization.

From this study, we were unable to delineate the correct degradation period of the GMSs in the vascular space. Although the obtained results were inconclusive with respect to the degradation period of GMSs, we observed some important characteristics of GMSs within the vascular space. First, it was confirmed that GMSs have the potential to degrade within vessels. As observed, in the cases where the GMSs were histologically identified within the vessels, the particles in all GMS groups degraded sequentially. Although the complete degradation period could not be obtained during the 14 days of observation, most of the GMS particles showed a high level of degradation after the 14-day observation period. It is speculated that the residual particles will degrade completely in the subsequent one or two weeks. Defining the exact degradation period within the vessel will require extended angiographic and

pathologic observations lasting for more than 14 days. Further, it was proven that GMSs could persist in the vessels for a longer period than that in the subcutaneous tissue. The reason is speculated as follows. Gelatin is known to be degraded by gelatin-degrading enzymes that are widely distributed in body fluids (24). If the GMSs are located within the subcutaneous tissue, they are easily accessible to the gelatin-degrading enzymes. In contrast, when the GMSs are impacted in the small vessels, particularly in the end arteries (as in this study), the blood flow is blocked; consequently, the interaction between the GMS particles and the enzymes would be disturbed. In order to prevent the occurrence of this phenomenon, an artery that is not categorized as an end artery should be used in an experimental study.

This study has the following limitations. First, the renal artery was considered because it can be easily cannulated and has a diameter suited to this experiment; however, as described previously, the TAE for the renal artery cannot be extrapolated to the general TAE for tumors, such as those of the liver or the pelvic organ, because it is an end artery without any collateral circulation. The occlusion of the renal artery induces renal infarction without exception, and this might influence the degradation period of the GMSs. Ideally, to evaluate both the degradation period and the embolic effect assuming a clinical condition, the hepatic or internal iliac artery should be considered because they are categorized as non-end arteries. However, it is technically difficult to perform an angiogram and embolization for the abovementioned arteries in the rabbit model. A larger animal model would be required for the execution of this experiment. Second, although three types of GMSs—35–100 μm , 100–200 μm , and 200–300 μm in size—were used in this study, many experimental results overlapped among the three groups. In order to accentuate the differences between the groups, the study should have been performed by narrowing the diameter range and considering sizes such as 35–45 μm , 100–120 μm , and 250–300 μm . Third, as described previously, although the GMSs were observed in the histological specimens on day 14 after the embolization, the degradation period of the GMSs within the vessels could not be precisely determined because the study was scheduled only for 14 days. To resolve this issue, the observation period should exceed 14 days.

From this study, it was confirmed that GMSs have sufficient potential to be used as embolic materials. If GMSs of various sizes and degradation periods are made commercially available in the future, a customized TAE procedure can be designed by changing the level and the period of occlusion.

References

1. Feldman F, Casarella WJ, Dick HM, Hollander BA. Selective intra-arterial embolization of bone tumors. A useful adjunct in the management of selected lesions. *Am J Roentgenol Radium Ther Nucl Med* 1975;123:130-139
2. Rosch J, Dotter CT, Brown MJ. Selective arterial embolization. A new method for control of acute gastrointestinal bleeding. *Radiology* 1972;102:303-306
3. Pugatch RD, Wolpert SM. Transfemoral embolization of an external carotid-cavernous fistula. Case report. *J Neurosurg* 1975;42:94-97
4. Kunstlinger F, Brunelle F, Chaumont P, Doyon D. Vascular occlusive agents. *AJR Am J Roentgenol* 1981;136:151-156
5. Spies JB, Benenati JF, Worthington-Kirsch RL, Pelage JP. Initial experience with use of tris-acryl gelatin microspheres for uterine artery embolization for leiomyomata. *J Vasc Interv Radiol* 2001;12:1059-1063
6. Jiaqi Y, Hori S, Minamitani K, Hashimoto T, Yoshimura H, Nomura N, et al. A new embolic material: super absorbent polymer (SAP) microsphere and its embolic effects. *Nippon Igaku Hoshasen Gakkai Zasshi* 1996;56:19-24
7. Coley SC, Jackson JE. Endovascular occlusion with a new mechanical detachable coil. *AJR Am J Roentgenol* 1998;171:1075-1079
8. Katsumori T, Nakajima K, Mihara T, Tokuhiko M. Uterine artery embolization using gelatin sponge particles alone for symptomatic uterine fibroids: midterm results. *AJR Am J Roentgenol* 2002;178:135-139
9. Sniderman KW, Sos TA, Alonso DR. Transcatheter embolization with Gelfoam and Avitene: the effect of Sotradecol on the duration of arterial occlusion. *Invest Radiol* 1981;16:501-507
10. Vlahos L, Benakis V, Dimakakos P, Dimopoulos C, Pontifex G. A comparative study of the degree of arterial recanalization in kidneys of dogs following transcatheter embolization with eight different materials. *Eur Urol* 1980;6:180-185
11. Tabata Y, Uno K, Ikada Y, Muramatsu S. Potentiation of antitumor activity of macrophages by recombinant interferon alpha A/D contained in gelatin microspheres. *Jpn J Cancer Res* 1988;79:636-646
12. Tabata Y, Ikada Y. Synthesis of gelatin microspheres containing interferon. *Pharm Res* 1989;6:422-427
13. Tabata Y, Uno K, Muramatsu S, Ikada Y. In vivo effects of recombinant interferon alpha A/D incorporated in gelatin microspheres on murine tumor cell growth. *Jpn J Cancer Res* 1989;80:387-393
14. Tabata Y, Miyao M, Inamoto T, Ishii T, Hirano Y, Yamaoki Y, et al. De novo formation of adipose tissue by controlled release of basic fibroblast growth factor. *Tissue Eng* 2000;6:279-289
15. Tabata Y, Hong L, Miyamoto S, Miyao M, Hashimoto N, Ikada Y. Bone formation at a rabbit skull defect by autologous bone marrow cells combined with gelatin microspheres containing TGF-beta1. *J Biomater Sci Polym Ed* 2000;11:891-901
16. Kushibiki T, Matsumoto K, Nakamura T, Tabata Y. Suppression of the progress of disseminated pancreatic cancer cells by NK4 plasmid DNA released from cationized gelatin microspheres. *Pharm Res* 2004;21:1109-1118
17. U.S. Food and Drug Administration, Gelfoam® Sterile Powder. Available at <http://www.fda.gov/cdrh/pdf/n18286s012.html> Accessed March 23, 2006
18. Correll JT, Prentice HR, Wise EC. Biologic investigations of a new absorbable sponge. *Surg Gynecol Obstet* 1945;81:585-589

19. Ozeki M, Tabata Y. In vivo degradability of hydrogels prepared from different gelatins by various cross-linking methods. *J Biomater Sci Polym Ed* 2005;16:549-561
20. Brown DB, Pilgram TK, Darcy MD, Fundakowski CE, Lisker-Melman M, Chapman WC, et al. Hepatic arterial chemoembolization for hepatocellular carcinoma: comparison of survival rates with different embolic agents. *J Vasc Interv Radiol* 2005;16:1661-1666
21. Jinbo G. *Science of Particles*. Tokyo: Kodansya, 1985;12-24
22. Theo G. M., van de Ven. *Classical DLVO theory*. In: Theo G. M., van de Ven eds. *Colloidal Hydrodynamics*. San Diego: Academic Press, 1989;39-41
23. Goldstein HM, Wallace S, Anderson JH, Bree RL, Gianturco C. Transcatheter occlusion of abdominal tumors. *Radiology* 1976;120:539-545
24. Tryggvason K, Huhtala P, Höyhty M, Hujanen E, Hurskainen T. 70 K type IV collagenase (gelatinase). *Matrix Suppl* 1992;1:45-50